Plasma screening and the critical end point in the QCD phase diagram

Alejandro Ayala
Instituto de Ciencias Nucleares,
Universidad Nacional Autónoma de México
In collaboration with B. Almeida, J.J. Cobos, S. Hernández,
L. Hernández, A. Raya, M.E Tejeda-Yeomans
e-Print:2108.02362 [hep-ph]

37th Winter Workshop on Nuclear Dynamics
Puerto Vallarta, México
March 2022

The QCD phase diagram

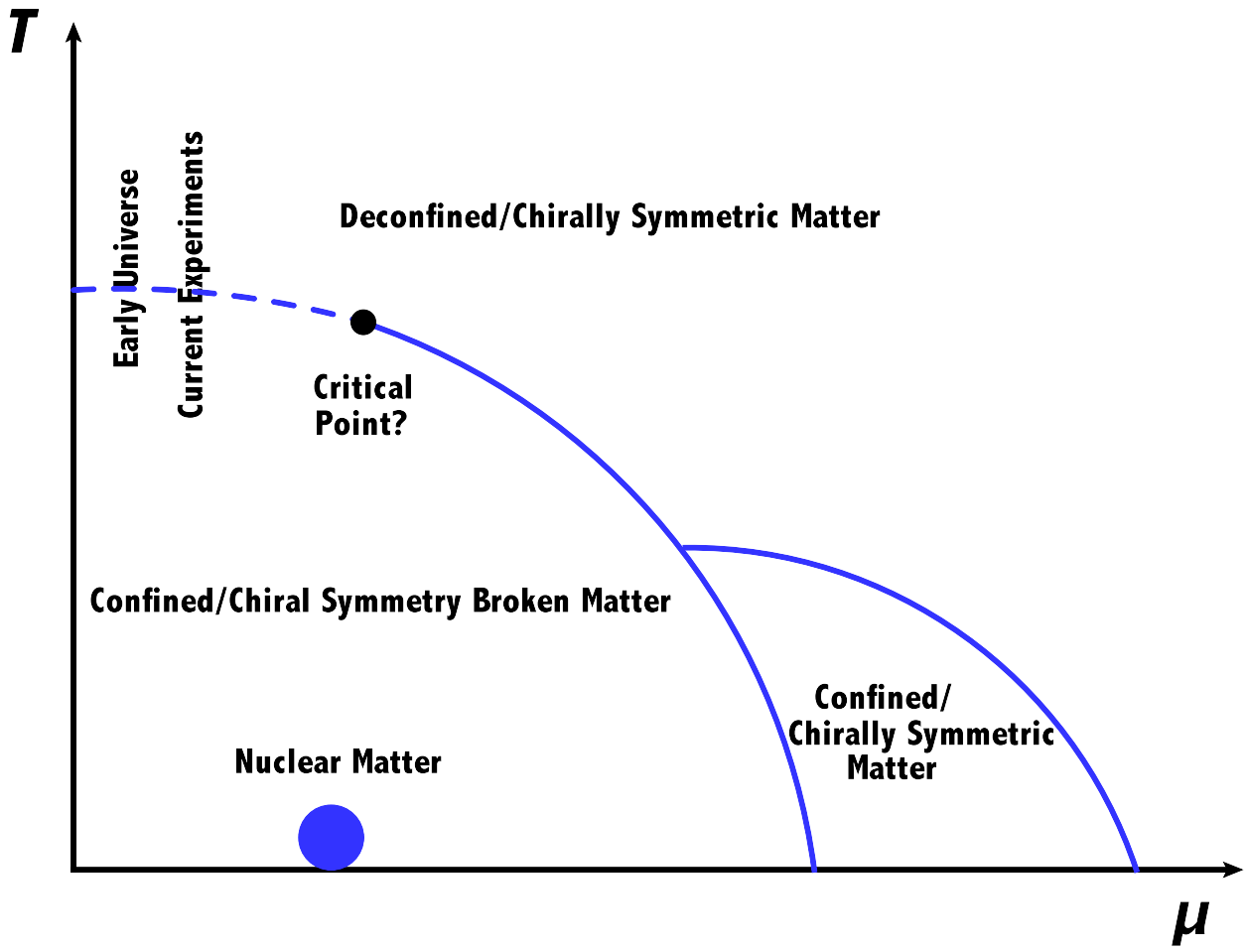

Motivation: Study fluctuations of conserved charges as a signature of the CEP

$$\kappa\sigma^2 = C_4/C_2$$

Model

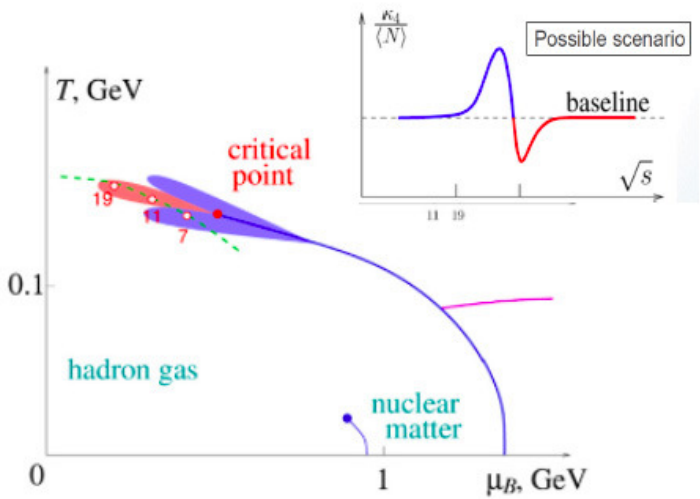

STAR BES Data

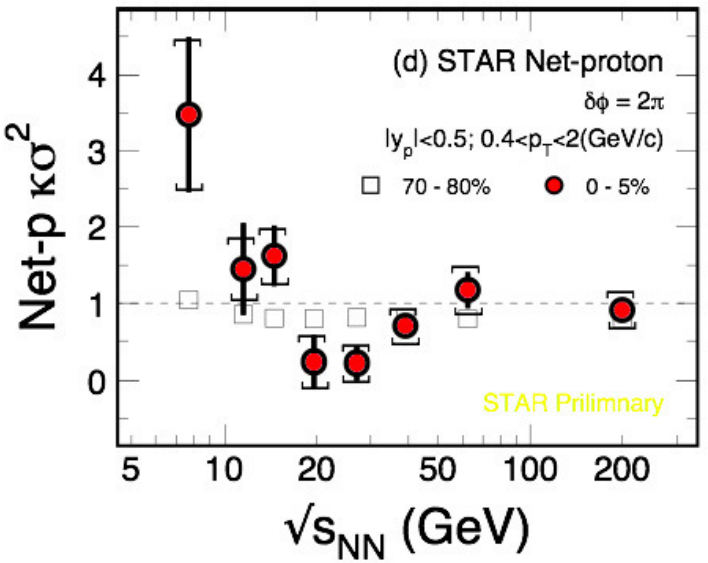

M.A. Stephanov, PRL107, 052301 (2011).
Schaefer&Wanger,PRD 85, 034027 (2012)
Vovchenko et al., PRC92, 054901 (2015)
JW Chen et al., PRD93, 034037 (2016)
arXiv: 1603.05198.

Non-monotonic energy dependence is observed for 4th order net-proton fluctuations in most central Au+Au collisions.

More recently: Yu Zhang, STAR Collaboration

Result 1: Net-proton C_4/C_2 from BES-I

J. Adam *et al.* (STAR Collaboration) Phys. Rev. Lett. **126**, 092301; long version paper: arXiv:2101.12413

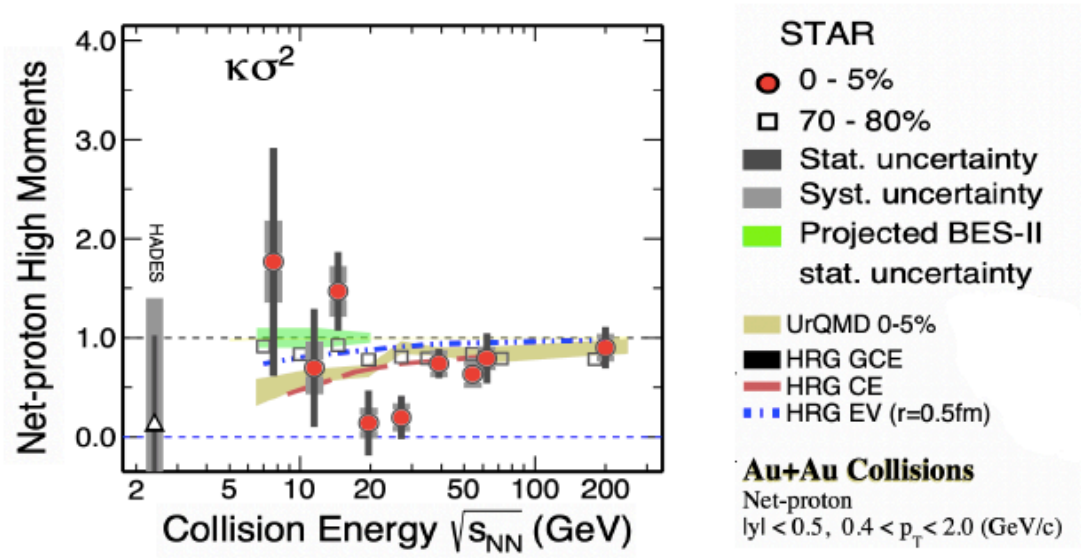

- Non-monotonic energy dependence of net-proton $\kappa\sigma^2$ is shown in top 5% from BES-I data which is not reproduced by various models.
- More statistics below 20 GeV are needed to confirm the non-monotonic trend.
- Measurement from new dataset in fixed target experiment at $\sqrt{s_{NN}} = 3$ GeV is on the way!

2021/4/2 55th Rencontres de Moriond 2021 10

QCD: The theory of strong interactions

$$\mathcal{L}_{QCD} = \sum_{i=1}^{N_f} \overline{\psi}_i^a \left(i\gamma^\mu (\partial_\mu \delta^{ab} + i g_s A_\mu^{ab}) - m_i \delta^{ab} \right) \psi_i^b - \frac{1}{4} G_{\mu\nu}^\alpha G_\alpha^{\mu\nu};$$

$$G_{\mu\nu}^\alpha = \partial_\mu A_\nu^\alpha - \partial_\nu A_\mu^\alpha + g_s f^{\alpha\beta\sigma} A_\mu^\beta A_\nu^\sigma; \qquad A_\mu^{ab} = A_\mu^\sigma (\tau_\sigma)^{ab}$$

a, b run from 1 to N_c, $\alpha,\ \beta,\ \sigma$ run from 1 to $N_c^2 - 1$.

- Gauge theory with the **local** symmetry group $SU(N_c)$. (In the real world $N_c = 3$).
- The fundamental fields are the **quarks** (matter fields) and **gluons** gauge fields.
- In the limit that each one of the N_f **quark fields** is massless ($m_i = 0$), QCD shows chiral symmetry.

The (bottom of the) Mexican ~~hat~~ glass potential

Spontaneous chiral symmetry breaking

$$\mathcal{L} = \frac{1}{2}(\partial_\mu \sigma)^2 + \frac{1}{2}(\partial_\mu \vec{\pi})^2 + \frac{a^2}{2}(\sigma^2 + \vec{\pi}^2) - \frac{\lambda}{4}(\sigma^2 + \vec{\pi}^2)^2; \quad \sigma \to \sigma + v$$

$$m_\sigma^2 = (3\lambda v^2 - a^2); \quad m_\pi^2 = (\lambda v^2 - a^2); \quad a^2 > 0$$

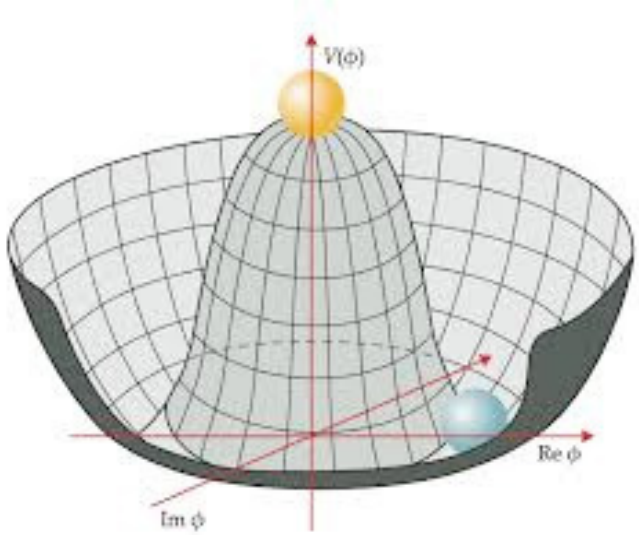

$$V^{\text{tree}}(v) = -\frac{a^2}{2}v^2 + \frac{\lambda}{4}v^4; \quad v_0 = \sqrt{\frac{a^2}{\lambda}}$$

Vacuum structure from would-be partition function

$$\mathcal{Z}(v) \sim \exp\left\{-V^{tree}(v)\right\}$$

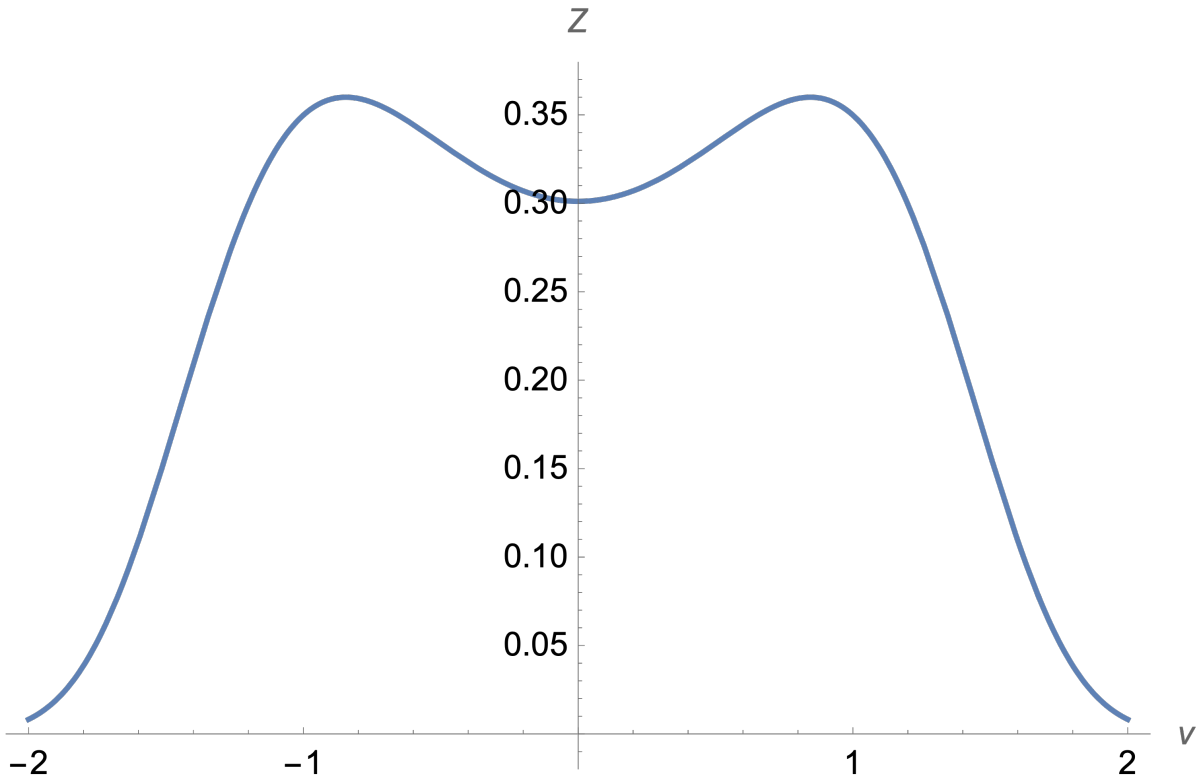

With one-loop thermal corrections

$$
\begin{aligned}
V^{\text{eff}} &= V^{\text{tree}} + V^{\text{b}} \\
V^{\text{tree}}(v) &= -\frac{a^2}{2}v^2 + \frac{\lambda}{4}v^4 \\
V^{\text{b}}(v,T) &= T\sum_n \int \frac{d^3k}{(2\pi)^3} \ln D_{\text{b}}(\omega_n, \vec{k})^{1/2} \\
V^{\text{eff}}(v) \quad \overrightarrow{\text{Large T}} \quad & -\frac{a^2}{2}v^2 + \frac{\lambda}{4}v^4 \\
&+ \sum_{\text{b}=\pi^{\pm},\pi^0,\sigma} \left\{ -\frac{T^4\pi^2}{90} + \frac{T^2 m_{\text{b}}^2}{24} - \frac{T m_{\text{b}}^3}{12\pi} - \frac{m_{\text{b}}^4}{64\pi^2} \ln\left(\frac{m_b^2}{T^2}\right) \right\}
\end{aligned}
$$

Troublesome when m_b^2 becomes 0 or even negative

Thermodynamics within a volume Ω from the effective potential

$$\mathcal{Z}(T, v) = \exp\left\{-\Omega V^{\text{eff}}(v)/T\right\}$$

Ideal gas with **classical** hadron thermodynamics

- Consider an ideal gas of identical neutral scalar particles of mass m_0 contained in a box volume Ω. To simplify assume Boltzmann statistics. The partition function is given by

$$\mathcal{Z}(T) = \sum_N \frac{1}{N!}\left[\frac{\Omega}{(2\pi)^3}\int d^3p \exp\left\{-\frac{\sqrt{p^2+m_0^2}}{T}\right\}\right]^N$$

$$\ln \mathcal{Z}(T) = \frac{\Omega T m_0^2}{2\pi^2} K_2(m_i/T)$$

$$\epsilon(T) = -\frac{1}{\Omega}\frac{\partial \ln \mathcal{Z}(T)}{\partial(1/T)} \overset{T\gg m_0}{\longrightarrow} \frac{3}{\pi^2}T^4 \quad \text{energy density}$$

$$n(T) = -\frac{1}{\Omega}\frac{\partial \ln \mathcal{Z}(T)}{\partial(\Omega)} \overset{T\gg m_0}{\longrightarrow} \frac{1}{\pi^2}T^3 \quad \text{particle density}$$

$$\omega(T) = \epsilon(T)/n(T) \simeq 3T \quad \text{average energy per particle}$$

Chiral transition and hadronization

- Hadron multiplicities established very close to the phase boundary.

Statistical model (Hadron Resonance Gas model)

$$n_j = \frac{g_j}{2\pi^2}\int_0^\infty p^2 dp \left[\exp\left\{\sqrt{p^2+M_j^2}/T_{\rm ch} - \mu_{\rm ch}\right\} \pm 1\right]^{-1}$$

- From the hadron side, abundances due to multi-particle collisions whose importance is **enhanced due to high particle density in the phase transition region.** Collective phenomena play an important role.
- **Since the multi-particle scattering rates fall-off rapidly, the experimentally determined chemical freeze-out is a good measure of the phase transition temperature.**

Chiral transition and hadronization

Chiral transition, hadronization and freeze-out

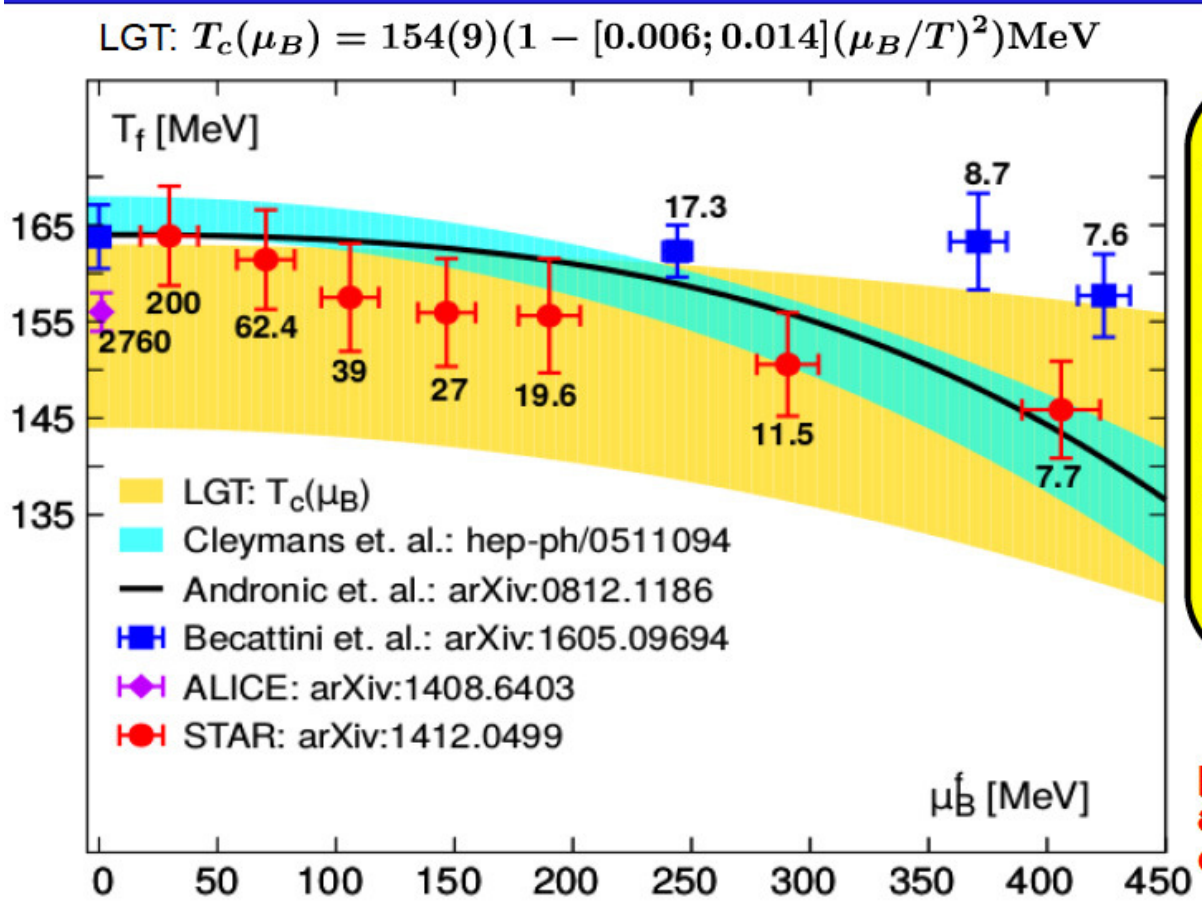

phenomenological freeze-out / hadronization curve, **QCD transition line** and experimental data (obtained by assuming the validity of the HRG model) are consistent for

$$\mu_B/T \lesssim 3$$

HOWEVER

physics is quite different at lower and upper end of the current error bar on Tc

⇒ **probed with net-charge correlations&fluctuations**

Analysis tools: Cumulant generating function

- The relation with thermodynamics comes through the partition function $\mathcal{Z}$, which is the fundamental object

The partition function is also the moment generating function and therefore **the cumulant generating function is given by** $\ln \mathcal{Z}$

- Cumulants are extensive quantities. Consider the number N of a conserved quantity in a volume Ω in a grand canonical ensemble. It can be shown that its cumulant of order n can be written as

$$\langle N^n \rangle_{c,\Omega} = \chi_n \Omega$$

χ_n are called the **generalized susceptibilities**

Susceptibilities

- Experimentally it is easier to measure the **central moments** M: $M^{ijk}_{BQS} = \langle (B - \langle B \rangle)^i (Q - \langle Q \rangle)^j (S - \langle S \rangle)^k \rangle$.
- On the other hand, derivatives of $\ln \mathcal{Z}$ with respect to the chemical potentials give the susceptibilities χ:

$$\chi^{ijk}_{BQS} = \frac{\partial^{i+k+j}(P/T^4)}{\partial^i(\mu_B/T)\partial^j(\mu_Q/T)\partial^k(\mu_S/T)}; \quad P = \frac{T}{\Omega} \ln \mathcal{Z}.$$

$$\Longrightarrow \chi_{XY} = \frac{1}{\Omega} T^3 M^{11}_{XY}$$

Analysis tools: Fluctuations of conserved quantities

- A powerful tool to experimentally locate the CEP is the study of **event-by-event fluctuations** in relativistic heavy-ion collisions

Fluctuations are sensitive to the early thermal properties of the created medium. **To locate the CEP, one looks for fluctuations that deviate from the ones that correspond to the HRGM**

Analysis tools: Cumulant generating function

Cumulants higher than second order vanish for a Gaussian probability distribution, non-Gaussian fluctuations are signaled by non-vanishing higher order cumulants

Two important higher order moments are the **skewness** S and the **curtosis** κ. The former measures the asymmetry of the distribution function whereas the latter measures its sharpness

Cumulants

For the HRGM,
ratios of cumulatns of even order are equal to 1

In particular, for the square of the variance σ^2 and the kurtosis κ

$$\langle N^4 \rangle_c / \langle N^2 \rangle_c = \kappa \sigma^2$$

Look for deviations from 1 in $\kappa\sigma^2$ as a function of collision energy as a signal of the CEP.

Linear sigma model with quarks

$$
\begin{aligned}
\mathcal{L} &= \frac{1}{2}(\partial_\mu\sigma)^2 + \frac{1}{2}(\partial_\mu\vec{\pi})^2 + \frac{a^2}{2}(\sigma^2+\vec{\pi}^2) \\
&- \frac{\lambda}{4}(\sigma^2+\vec{\pi}^2)^2 + i\bar{\psi}\gamma^\mu\partial_\mu\psi - g\bar{\psi}(\sigma + i\gamma_5\vec{\tau}\cdot\vec{\pi})\psi, \\
\sigma &\to \sigma + v \\
\mathcal{L} &= \frac{1}{2}(\partial_\mu\sigma)^2 + \frac{1}{2}(\partial_\mu\vec{\pi})^2 - \frac{1}{2}\left(3\lambda v^2 - a^2\right)\sigma^2 \\
&- \frac{1}{2}\left(\lambda v^2 - a^2\right)\vec{\pi}^2 \\
&+ \frac{a^2}{2}v^2 - \frac{\lambda}{4}v^4 + i\bar{\psi}\gamma^\mu\partial_\mu\psi - gv\bar{\psi}\psi + \mathcal{L}_I^b + \mathcal{L}_I^f \\
\mathcal{L}_I^b &= -\frac{\lambda}{4}\Big[(\sigma^2+(\pi^0)^2)^2 + 4\pi^+\pi^-(\sigma^2+(\pi^0)^2+\pi^+\pi^-)\Big], \\
\mathcal{L}_I^f &= -g\bar{\psi}(\sigma + i\gamma_5\vec{\tau}\cdot\vec{\pi})\psi
\end{aligned}
$$

Effective potential

$$
\begin{aligned}
V^{\text{eff}} &= V^{\text{tree}} + V^{\text{b}} + V^{\text{f}} + V^{\text{Ring}} \\
V^{\text{tree}}(v) &= -\frac{a^2}{2}v^2 + \frac{\lambda}{4}v^4 \\
V^{\text{b}}(v,T) &= T\sum_n \int \frac{d^3k}{(2\pi)^3} \ln D_{\text{b}}(\omega_n, \vec{k})^{1/2} \\
V^{\text{f}}(v,T,\mu) &= -T\sum_n \int \frac{d^3k}{(2\pi)^3} \text{Tr}[\ln S_{\text{f}}(\tilde{\omega}_n, \vec{k})^{-1}] \\
V^{\text{Ring}}(v,T,\mu) &= \frac{T}{2}\sum_n \int \frac{d^3k}{(2\pi)^3} \ln[1 + \Pi_{\text{b}} D(\omega_n, \vec{k})] \\
\Pi_{\text{b}} &\equiv \Pi_\sigma = \Pi_{\pi^\pm} = \Pi_{\pi^0} \\
&= \lambda\frac{T^2}{2} - N_{\text{f}}N_{\text{c}}g^2\frac{T^2}{\pi^2}\left[\text{Li}_2\left(-e^{-\frac{\mu}{T}}\right) + \text{Li}_2\left(-e^{\frac{\mu}{T}}\right)\right]
\end{aligned}
$$

Plasma screening in TFT: Ring diagrams

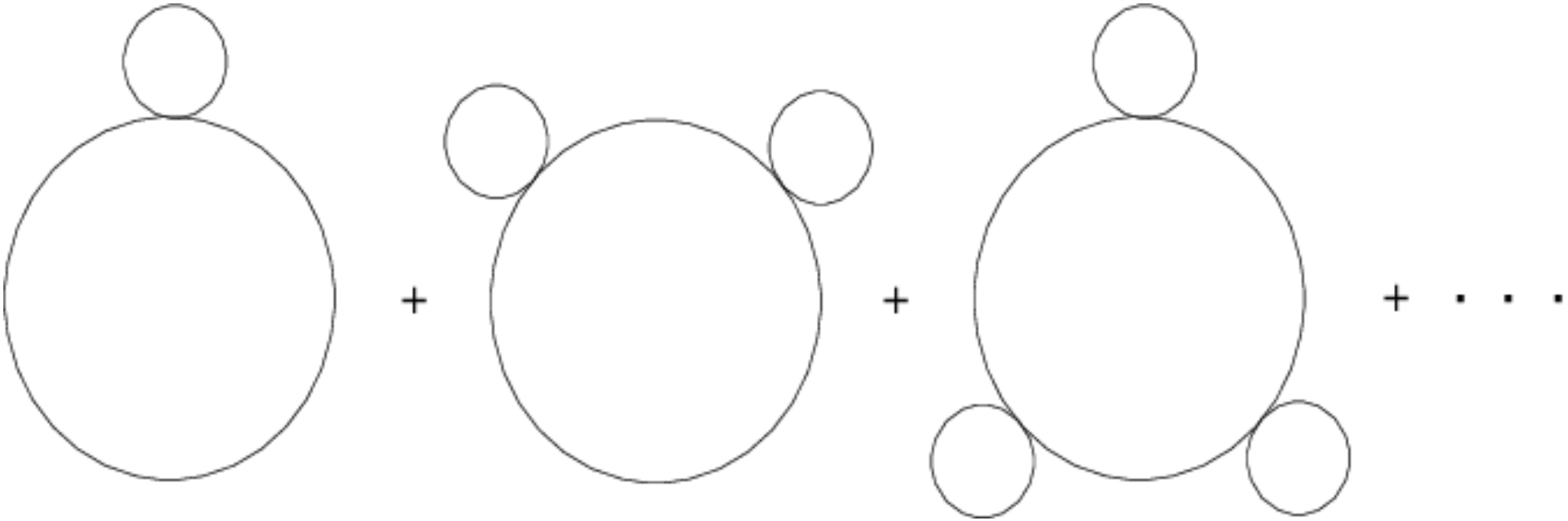

Effective potential

$$
\begin{aligned}
V^{\text{eff}}(v) &= -\frac{a^2}{2}v^2 + \frac{\lambda}{4}v^4 \\
&+ \sum_{\mathrm{b}=\pi^{\pm},\pi^0,\sigma} \left\{ -\frac{T^4\pi^2}{90} + \frac{T^2 m_{\mathrm{b}}^2}{24} - \frac{T(m_{\mathrm{b}}^2+\Pi_{\mathrm{b}})^{3/2}}{12\pi} \right. \\
&- \left. \frac{m_{\mathrm{b}}^4}{64\pi^2}\ln\left(\frac{\tilde{\mu}^2}{T^2}\right) \right\} \\
&+ N_{\mathrm{c}}N_{\mathrm{f}} \left\{ \frac{m_f^4}{16\pi^2} \left[\ln\left(\frac{\tilde{\mu}^2}{T^2}\right) - \psi^0\left(\frac{1}{2}+\frac{i\mu}{2\pi T}\right) - \psi^0\left(\frac{1}{2}-\frac{i\mu}{2\pi T}\right) \right. \right. \\
&+ \left. \left. \psi^0\left(\frac{3}{2}\right) - 2\left(1+\ln(2\pi)\right) + \gamma_E \right] \right. \\
&- \left. \frac{m_{\mathrm{f}}^2 T^2}{2\pi^2}\left[\mathrm{Li}_2\left(-e^{-\frac{\mu}{T}}\right) + \mathrm{Li}_2\left(-e^{\frac{\mu}{T}}\right) \right] \right. \\
&+ \left. \frac{T^4}{\pi^2}\left[\mathrm{Li}_4\left(-e^{-\frac{\mu}{T}}\right) + \mathrm{Li}_4\left(-e^{\frac{\mu}{T}}\right) \right] \right\}
\end{aligned}
$$

Fixing the parameters a^2, λ and g from LQCD Phys. Rev. Lett.125, 052001 (2020)

At the phase transition, the effective potential is flat at $v = 0$. This property can be exploited to find the suitable values of the model parameters a, λ and g at the critical temperature T_c for $\mu_B = 0$

$$6\lambda\left(\frac{T_c^2}{12} - \frac{T_c}{4\pi}\left(\Pi_b(T_c, \mu_B = 0) - a^2\right)^{1/2} + \frac{a^2}{16\pi^2}\left[\ln\left(\frac{\tilde{\mu}^2}{T_c^2}\right)\right]\right) + g^2 T_c^2 - a^2 = 0.$$

$$\frac{T_c(\mu_B)}{T_c} = 1 - \kappa_2\left(\frac{\mu_B}{T_c}\right)^2 + \kappa_4\left(\frac{\mu_B}{T_c}\right)^4,$$

Effective potential

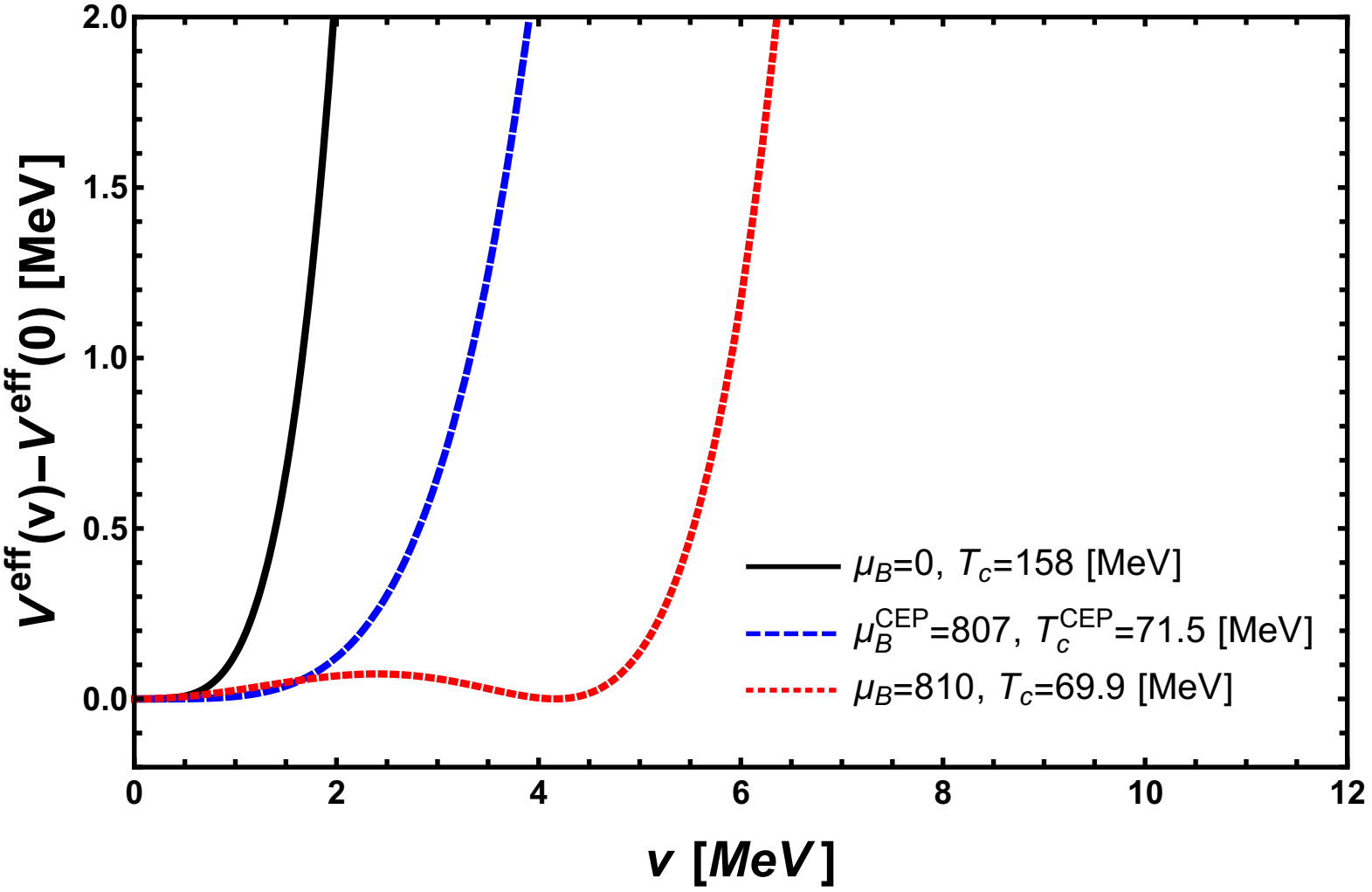

Partition function in the LSMq up to ring diagram order

$$\mathcal{Z}(v) = \exp\left\{-\Omega V^{\text{eff}}(v)/T\right\}$$

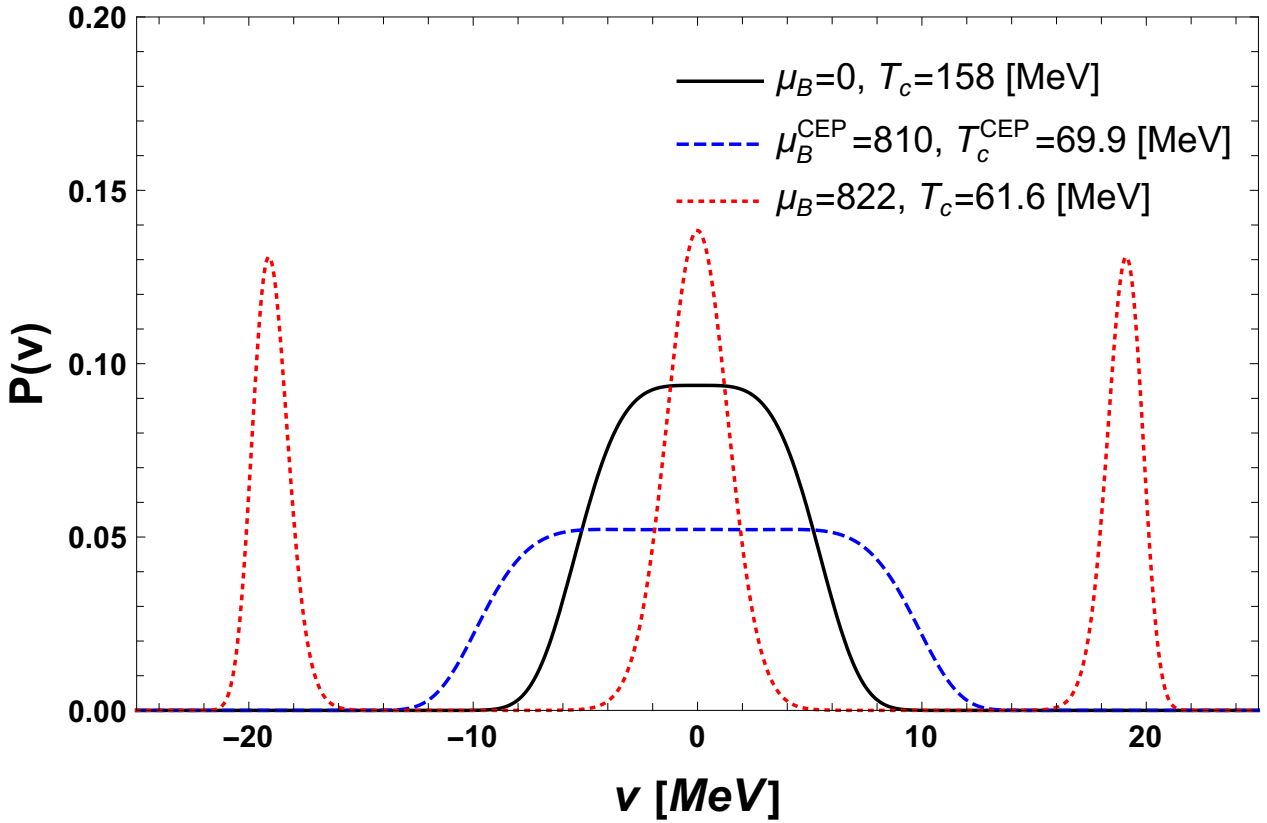

Baryon number fluctuations in the LSMq up to ring diagram order; curtosis

$$\mathcal{Z}(v) = \exp\left\{-\Omega V^{\text{eff}}(v)/T\right\}$$

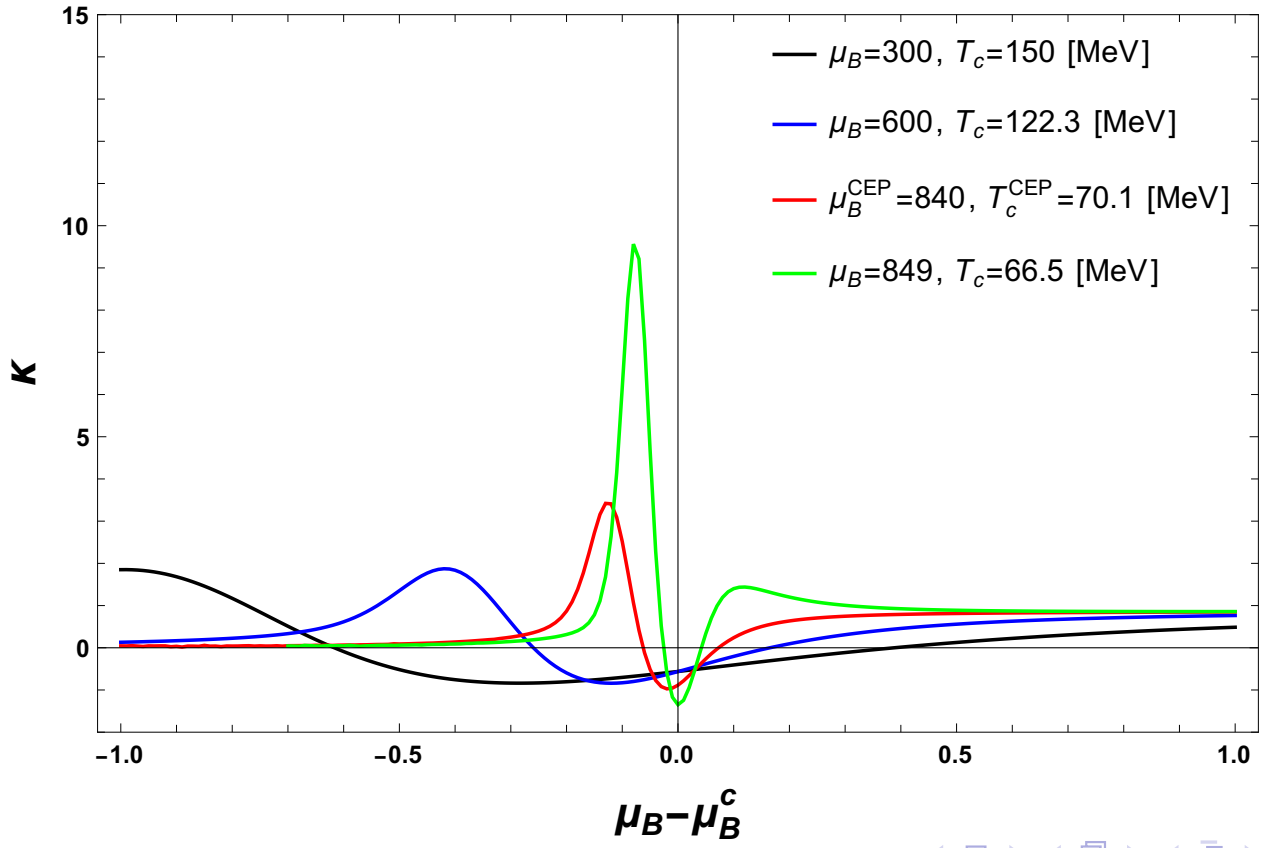

Effective phase diagram

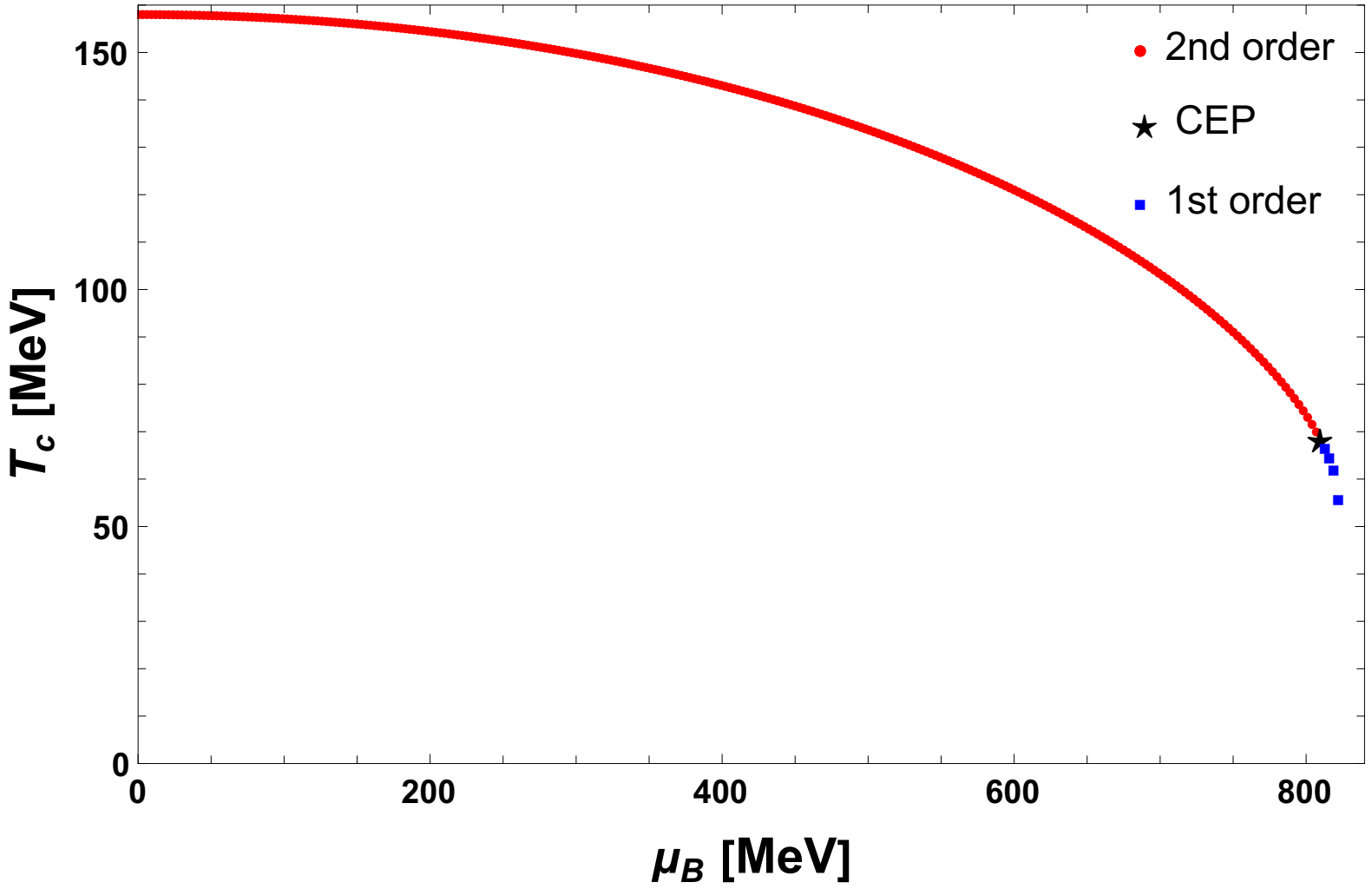

Freeze-out line Randrup & Cleymans, PRC **74**, 047901 (2006)

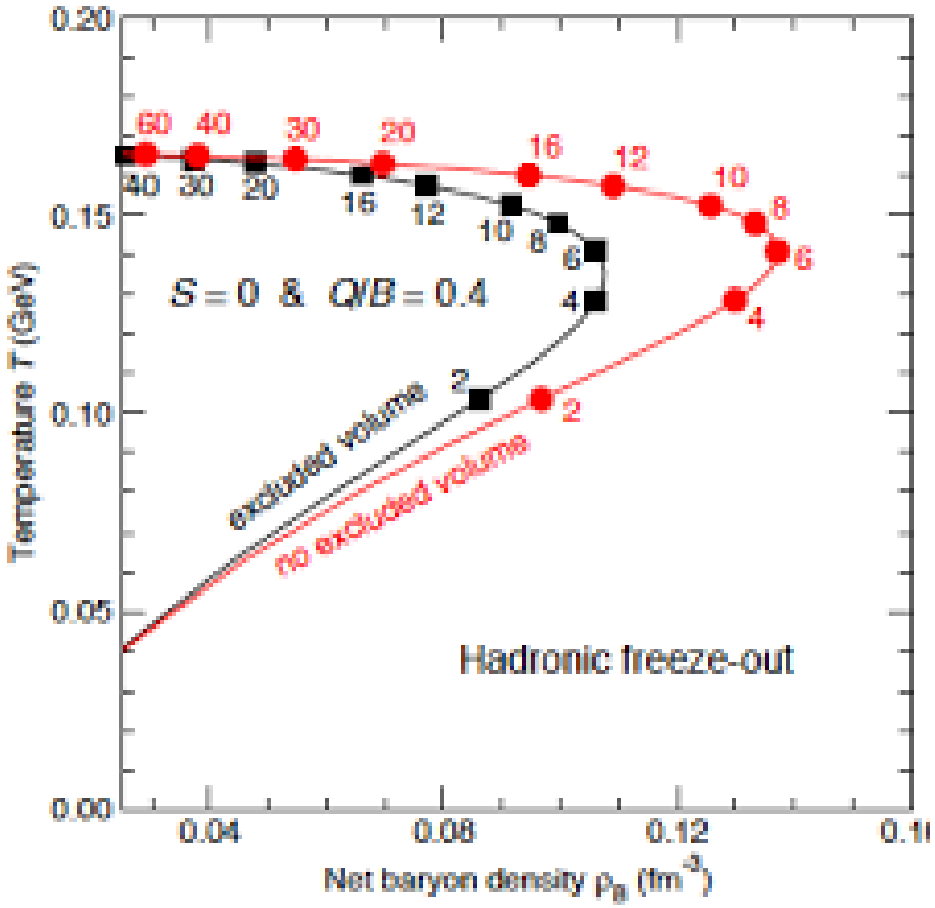

$$\mu_B(\sqrt{s_{NN}}) = \frac{d}{1 + e\sqrt{s_{NN}}} \quad d = 1.308\text{GeV}, \; e = 0.273\text{GeV}^{-1}$$

Baryon number fluctuations in the LSMq

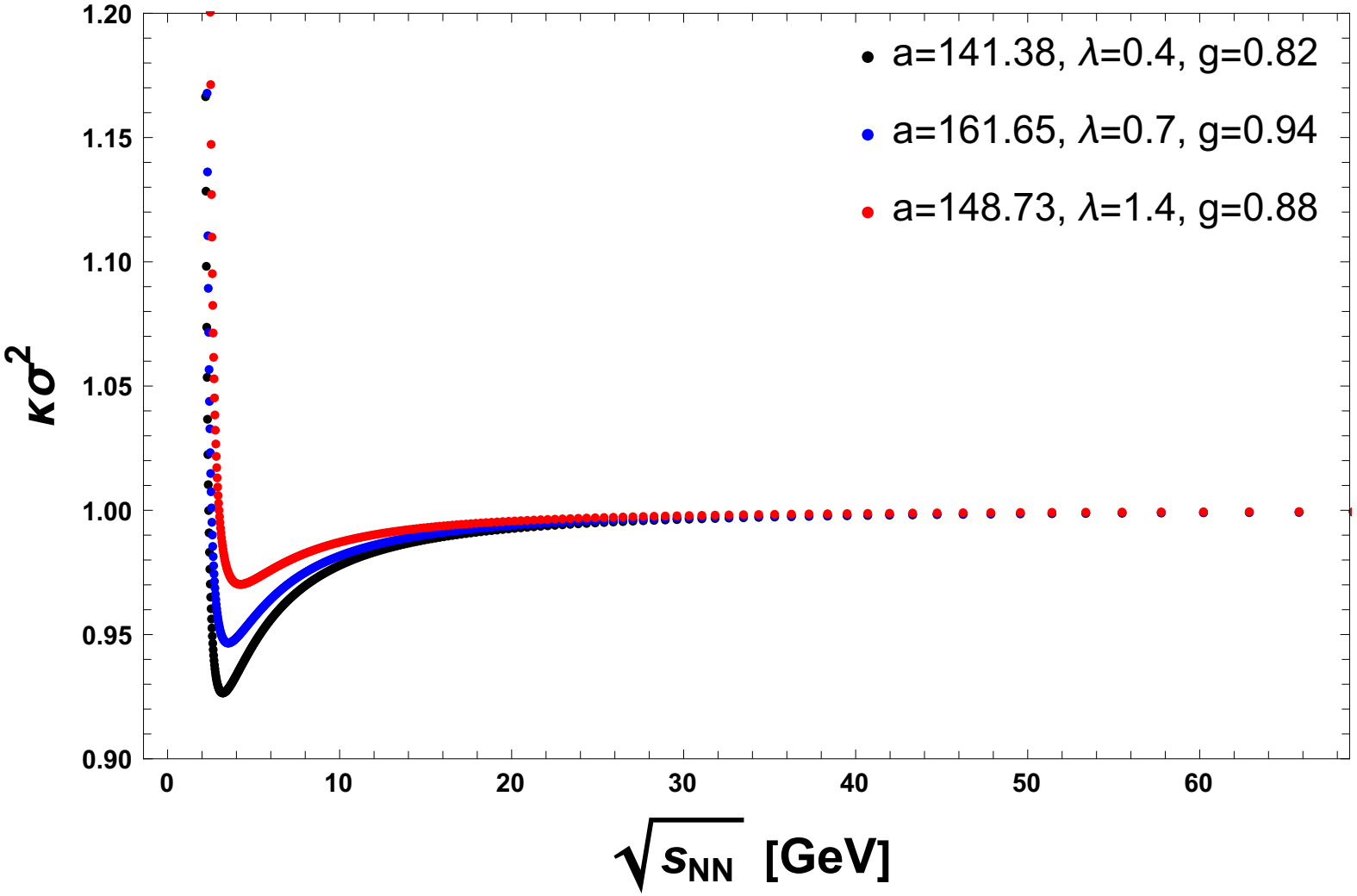

Summary

- Deviations from HRG behavior when using LSMq as an effective QCD model up to **ring diagrams contribution.**
- Ring diagrams inclusion is equivalent to introducing screening effects at finite T and μ_B.
- CEP signaled by divergence of $\kappa\sigma^2$
- 786 MeV $< \mu_B^{\text{CEP}} <$ 849 MeV and $T^{\text{CEP}} \sim$ 70.3 MeV
- CEP found at low T and high μ_B (NICA, HADES?)

¡Muchas Gracias!

BACKUP

Analysis tools: Fluctuations of conserved quantities

- For a probability distribution function $\mathcal{P}(x)$ of an stochastic variable x, the moments are defined as

$$\langle x^n \rangle = \int dx\, x^n \mathcal{P}(x)$$

- We can define the **moment generating function** $G(\theta)$ as

$$G(\theta) = \int dx\, e^{x\theta} \mathcal{P}(x)$$

- from where

$$\langle x^n \rangle = \frac{d^n}{d\theta^n} G(\theta)\Big|_{\theta=0}$$

Analysis tools: Cumulant generating function

$$K(\theta) = \ln G(\theta)$$

- The cumulants of $\mathcal{P}(x)$ are defined by

$$\begin{aligned}
\langle x^n \rangle_c &= \left. \frac{d^n}{d\theta^n} K(\theta) \right|_{\theta=0}, \\
\langle x \rangle_c &= \langle x \rangle, \\
\langle x^2 \rangle_c &= \langle x^2 \rangle - \langle x \rangle^2 = \langle \delta x^2 \rangle, \\
\langle x^3 \rangle_c &= \langle \delta x^3 \rangle, \\
\langle x^4 \rangle_c &= \langle \delta x^4 \rangle - 3 \langle \delta x^2 \rangle^2.
\end{aligned}$$

Analysis tools: Fluctuations of conserved quantities

- For example, the variance of Q is given

$$\langle \delta Q^2 \rangle_\Omega = \langle (Q - \langle Q \rangle_V)^2 \rangle_\Omega = \int_V dx_1 dx_2 \langle \delta n(x_1) \delta n(x_2) \rangle$$

- The integrand on the right-hand side is called a **correlation function**, whereas the left-hand side is called a (second order) **fluctuation**

We see that fluctuations are closely related to correlation functions

In relativistic heavy-ion collisions, fluctuations are measured on an event-by-event basis in which the number of some charge or particle species is counted in each event

Higher moments, larger sensitivity to correlation length ξ

- In HIC's, the simplest measurements of fluctuations are event-by-event variances in observables such as multiplicities or mean transverse momenta of particles.
- At the CEP, these variances diverge approximately as ξ^2. **They manifest as a non-monotonic behavior as the CEP is passed by during a beam energy scan.**
- In a realistic HIC, the divergence of ξ is tamed by the effects of *critical slow down* (the phenomenon describing a finite and possibly large relaxation time near criticality).
- However, higher, non-Gaussian moments of the fluctuations depend much more sensitively on ξ.
- **Important to look at the Kurtosis κ (proportional to the fourth-order cumulant C_4), which grows as ξ^7.**